Radio interferometry in astronomy: a view into the XXI century

Lecture 1

Introduction and basics of (radio) interferometry

Leonid Gurvits

JOINT INSTITUTE FOR VLBI IN EUROPE

Joint Institute for VLBI in Europe, Dwingeloo, The Netherlands

TU Delft

Delft University of Technology, Faculty of Aerospace Engineering, The Netherlands

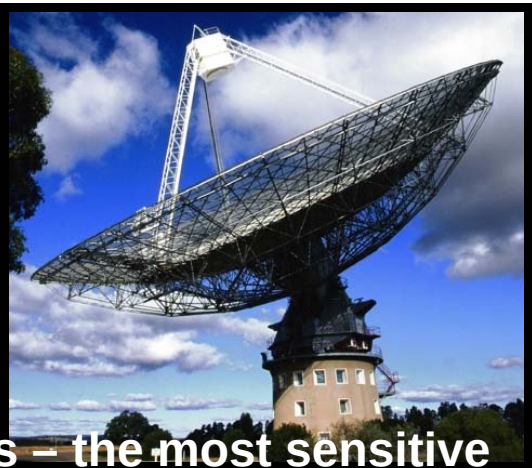

Radio telescopes – the most sensitive detectors of electro-magnetic waves

80 years of Radio astronomy

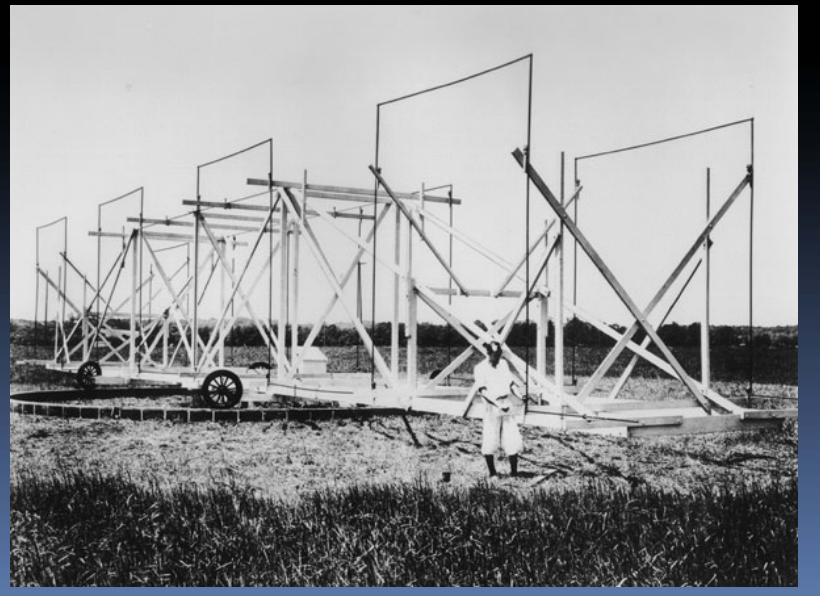

"Chance" discovery of cosmic radio emission by Karl Jansky, 1933

The beginning: 05 May 1933


"All the News That's Fit to Print."

The New York Times.

LATE CITY EDITION

VOL. LXXXII....No. 27,495. NEW YORK, FRIDAY, MAY 5, 1933.

NEW RADIO WAVES TRACED TO CENTRE OF THE MILKY WAY

Mysterious Static, Reported by K. G. Jansky, Held to Differ From Cosmic Ray.

Flier Asks Blame in Crash, But Inquest Absolves Him

BIG NEW INVASION PLANNED BY JAPAN ON ROAD TO PEIPING

League Reserve Cut Million By Drop in Dollar Value

ROOSEVELT ASKS PAY RISE FOR WORKERS; PROMISES TO HELP BUSINESS END CHAOS; HE SENDS RAILROAD BILL TO CONGRESS

Features of Railroad Bill

PRESIDENT TELLS OF GAINS

KIDNAPPERS URGED TO ANSWER PLEAS

FARM BILL CLAUSE BLOCKS AGREEMENT

Nazis Plan Demonstration on the Rhine; Border Incidents Already Alarm French


Karl Jansky


"All the News That's Fit to Print."

The New York Times.

Copyright, 1933, by The New York Times Company.

VOL. LXXXII....No. 27,495. Entered as Second-Class Matter, Postoffice, New York, N. Y. NEW YORK, FRIDAY, MAY 5,

NEW RADIO WAVES TRACED TO CENTRE OF THE MILKY WAY

Mysterious Static, Reported by K. G. Jansky, Held to Differ From Cosmic Ray.

Flier Asks Blame in Crash, But Inquest Absolves Him

BIG NEW INVASION PLANNED BY JAPAN ON ROAD TO PEIPING

Larger-Scale Offensive Than Last Is Announced to Open Soon in North China.

CHIANG RUSHES AID NORTH

Famous Units That Fought at Shanghai Are Dispatched to Help 50,000 at Front.

League Reserve Cut Million By Drop in Dollar Value

Let's be acquainted…

Joint Institute for VLBI in Europe

- **Founded in 1993 as a central institute of the European VLBI (Very Long Baseline Interferometry) Network (EVN);**
- **EVN unifies 14 institutes in 12 countries;**
- **JIVE develops and operates the EVN Data Processor – a purpose-built digital facility (correlator), the world most advanced VLBI data processor;**
- **JIVE provides to the world-wide community of VLBI observers (“users”)**
- **JIVE staff conduct cutting edge research in astrophysics and space science**

JIVE: areas of expertise

- **State-of-the-art data processing of (very large) data streams (~20 Gbit/s, multi Tbit/experiment)**
- **Operations and management of (globally) distributed networks of radio astronomy facilities**
- **Astrophysics and Space Science**
- **Management of (large) international collaborations (incl. FP 2-7 projects)**

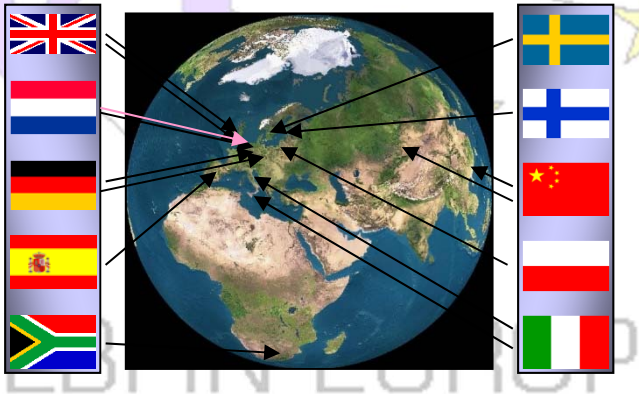

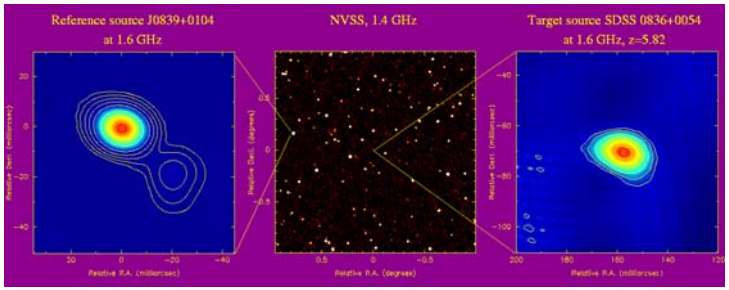

EVN & JIVE: user-oriented facility

- **Science done by world-wide user community**
  - "Open sky" policy
  - Access to the EVN via peer-reviewed proposals
  - Access by European users supported via EC FP7 programme RadioNet

- **JIVE provides support to (potential) users**
  - Proposals
  - Observations
  - Data processing
  - ***Users are NOT supposed to be "black-belt" VLBIers!***

- **New users are most welcome!**

The European VLBI Network

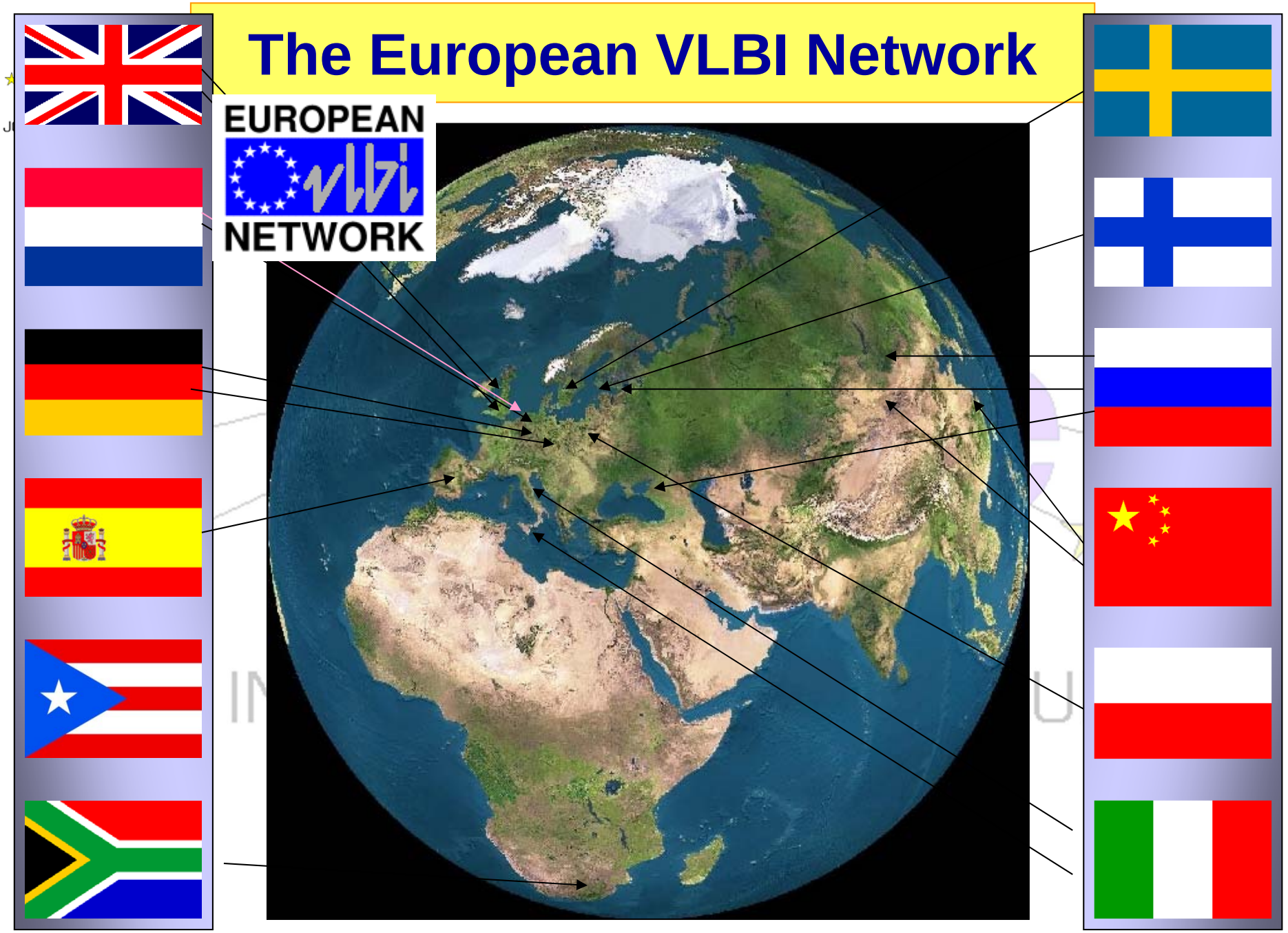

JOINT INSTITUTE FOR VLBI IN EUROPE

JIVE smiles 2011

In lieu of self-introduction

- **1973-1979**: Aerospace Engineering,
  (Spaceflight Control & Dynamics)
  Moscow Aviation Institute
- **1975-1979**: Astrophysics,
  Moscow State University
- **1979-1990**: Dept of Astrophysics,
  Space Research Institute, Moscow
- **1990-1992**: Astro Space Center,
  Lebedev Physical Institute, Moscow
- **1992-1994**: NAIC, Arecibo Observatory
  Cornell University, Puerto Rico
- **Since 1994**: Joint Institute for VLBI in Europe
- **Since 2011:** Faculty of Aerospace Engineering,
  Delft University of Technology

A glimpse of interferometry

Radio interferometry: a one-slide tutorial

- Michelson & Young, 1890's: measurements of stars' diametres
- Synthesis of large apertures *(by poor and curious people)*

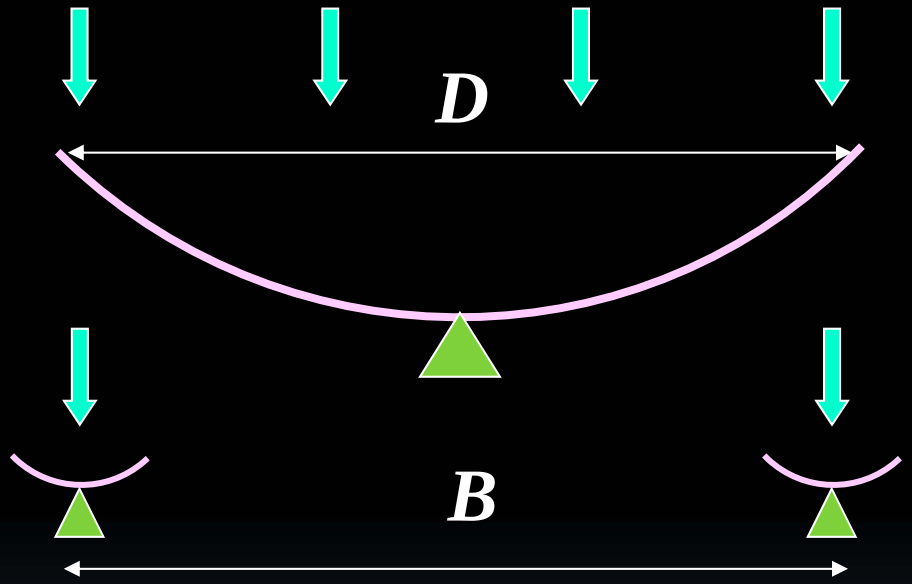

$$\vartheta = \frac{\lambda}{D}$$

Large aperture –
high sensitivity

$$\vartheta = \frac{\lambda}{B}$$

Large size –
high angular resolution

Very Long Baseline Interferometry (VLBI) - the ultimate angular resolution
- baselines up to 200,000 km

Young's double-slit interferometer, 1895

13.2. Young's Experiment. The original experiment performed by Young is shown schematically in Fig. 13*C*. Sunlight was first allowed to pass through a pinhole S and then, at a considerable distance away, through two pinholes S_1 and S_2. The two sets of spherical waves emerging from the two holes interfered with each other in such a way as to form a symmetrical pattern of varying intensity on the screen AC. Since

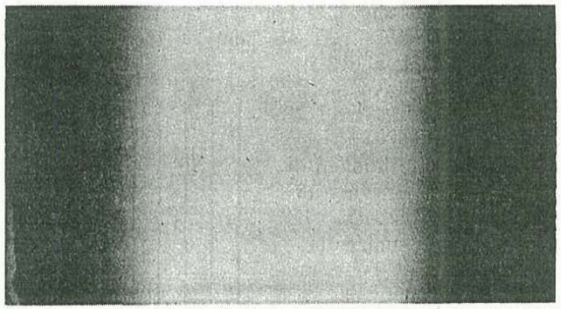

FIG. 13*B*. Photograph of the diffraction of light from a slit of width 0.001 mm.

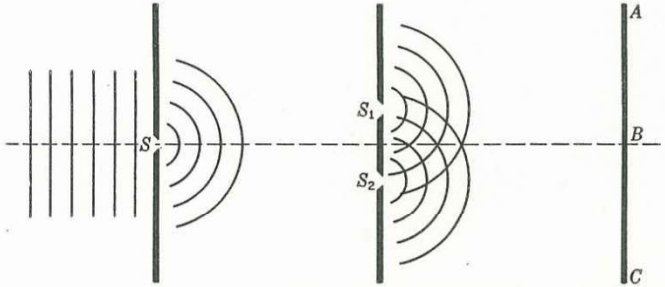

FIG. 13*C*. Experimental arrangement for Young's double-slit experiment.

this early experiment was performed, it has been found convenient to replace the pinholes by narrow slits and to use a source giving monochromatic light, i.e., light of a single wavelength. In place of spherical wave fronts we now have cylindrical wave fronts, represented equally well in two dimensions by the same Fig. 13*C*. If the circular lines represent crests of waves, the intersections of any two lines represent the arrival at those points of two waves with the same phase or with phases differing by a multiple of 2π. Such points are therefore those of maximum disturbance or brightness. A close examination of the light on the screen

will reveal evenly spaced light and dark bands or fringes, similar to those shown in Fig. 13*D*. Such photographs are obtained by replacing the screen AC of Fig. 13*C* by a photographic plate.

A very simple demonstration of Young's experiment can be accomplished in the laboratory or lecture room by setting up a single-filament lamp L (Fig. 13*E*) at the front of the room. The straight vertical filament S acts as the source and first slit. Double slits for each observer can be easily made from small photographic plates about 1 to 2 in.

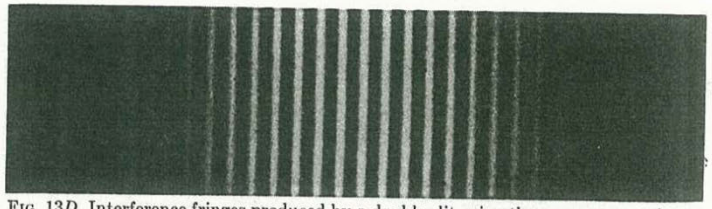

FIG. 13*D*. Interference fringes produced by a double slit using the arrangement shown in Fig. 13*C*.

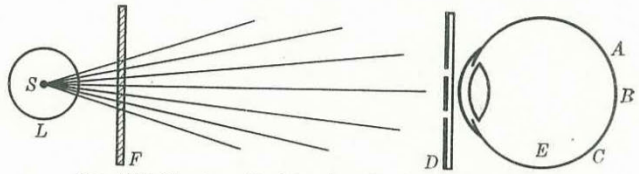

FIG. 13*E*. Simple method for observing interference fringes.

square. The slits are made in the photographic emulsion by drawing the point of a penknife across the plate, guided by a straight edge. The plates need not be developed or blackened but can be used as they are. The lamp is now viewed by holding the double slit D close to the eye E and looking at the lamp filament. If the slits are close together, e.g., 0.2 mm apart, they give widely spaced fringes, whereas slits farther apart, e.g., 1 mm, give very narrow fringes. A piece of red glass F, placed adjacent to and above another of green glass in front of the lamp, will show that the red waves produce wider fringes than the green, which we shall see is due to their greater wavelength.

Frequently one wishes to perform accurate experiments by using more nearly monochromatic light than that obtained by white light and a red or green glass filter. Perhaps the most convenient method is to use the sodium arc now available on the market, or a mercury arc plus a filter to isolate the green line, $\lambda 5461$. A suitable filter consists of a combination

Young's experiment 100 years later…

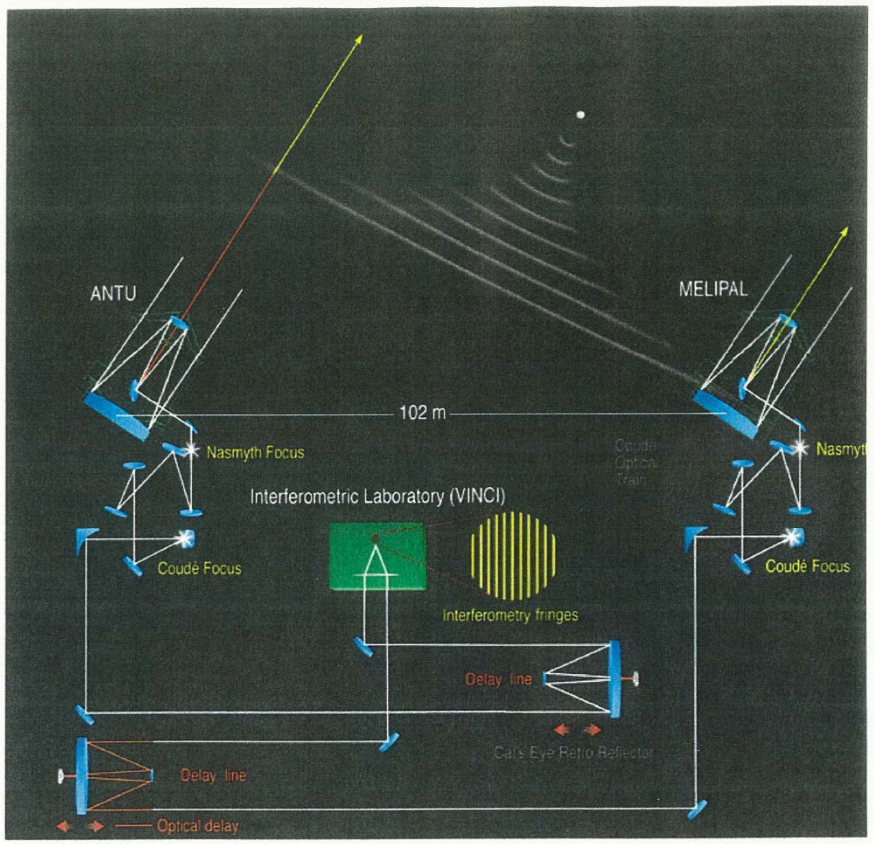

The VLT Interferometer with ANTU and MELIPAL

ESO PR Photo 30a/01 (5 November 2001) ©European Southern Observatory

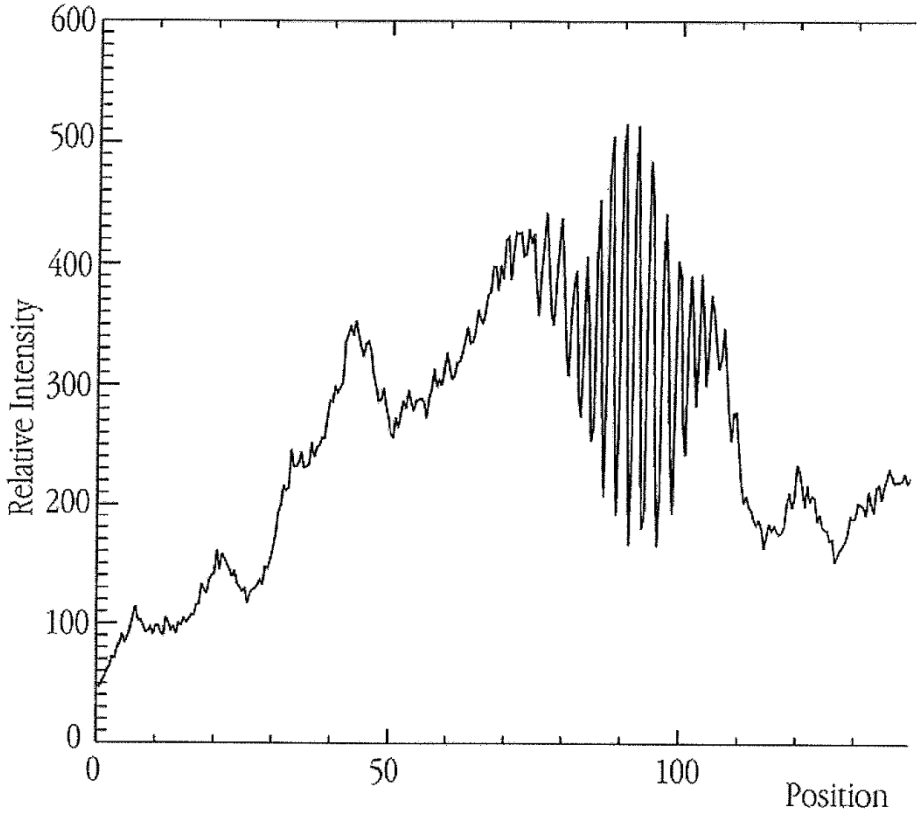

Interferometric Fringes of Achernar
(VLTI with ANTU and MELIPAL + VINCI)

ESO PR Photo 30c/01 (5 November 2001) ©European Souther

Intereferometer fundamentals

single point source

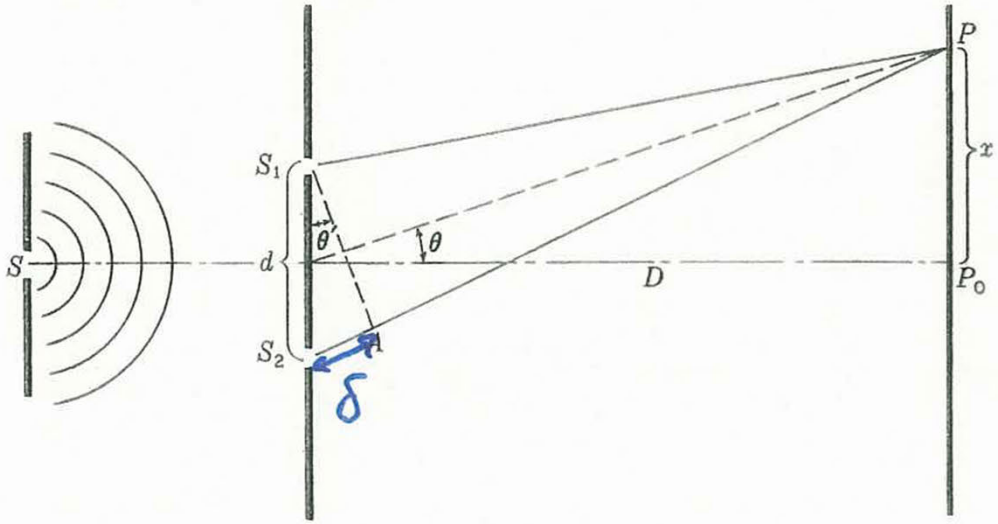

Path difference in Young's experiment.

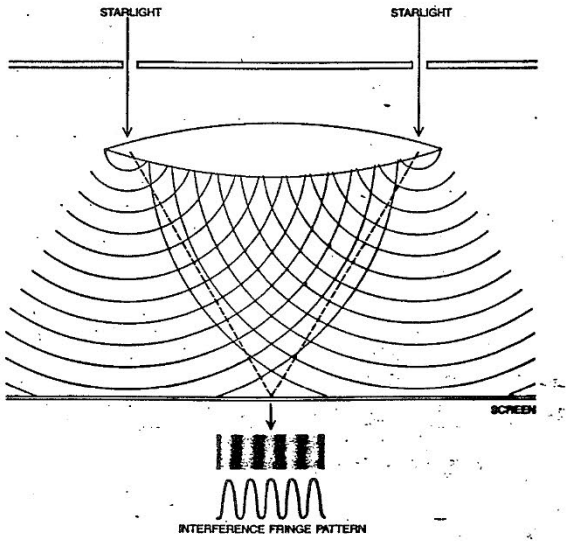

constructive interference: $\delta = n\lambda$

destructive interference: $\delta = (2n+1)\lambda/2$

n = 0,1,2,.....

Maxima in the fringe pattern are separated by λ/d (FRINGE SPACING)

History of radio interferometry (a subjective view)

1801	Young: double slit experiment
1890/1920	Michelson (+ Pease): optical interferometer
1887	Hertz: discovery of radio waves
1931	Jansky: discovery of cosmic radio radiation
1946	Ryle and Vonberg: radio analogue of Michelson interferometer
1948	Bolton and Stanley: sea-cliff interferometer
1952	Ryle: phase-switched interferometer
1955	Christiansen and Warburton: earth-rotation aperture synthesis
1955	Dwingeloo telescope
1962	Cambridge 1-mile telescope
1965	Mills Cross telescope
1967	Brown et al, Broten et al, Bare et al: VLBI
1970	Westerbork Synthesis Radio Telescope
1976	US VLBI Network
1980	European VLBI Network (EVN)
1982	VLA
1993	VLBA
1997	Space VLBI: VSOP / HALCA launched
1998	Joint Institute for VLBI in Europe (JIVE)
2003	First VLBI experiments with data transport via optical fibre networks

Sea interferometer

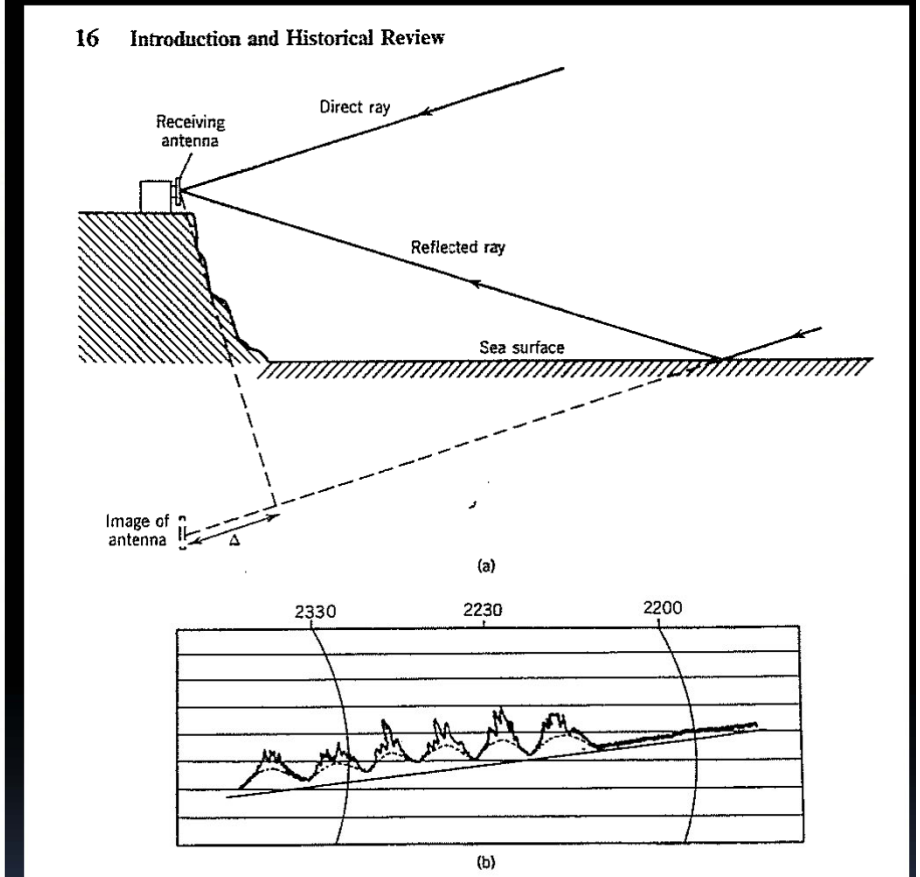

Figure 1.7 (a) Schematic diagram of a sea interferometer. The fringe pattern is similar to that which would be obtained with the actual receiving antenna and one at the position of its image in the sea. The reflected ray undergoes a phase change of 180° on reflection and travels an extra distance Δ in reaching the receiving antenna. (b) Sea interferometer record of the source Cygnus A at 100 MHz by Bolton and Stanley (1948). The source rose above the horizon at approximately 22.17. The broken line was inserted to show that the record could be interpreted in terms of a steady component and a fluctuating component of the source: the fluctuations were later shown to be of ionospheric origin. The fringe width was approximately 1.0° and the source was unresolved. Part (b) is reprinted by permission from *Nature*, Vol. 161, No. 4087, p. 313; copyright © 1948 Macmillan Journals Limited.

From interferometer to aperture synthesis

Earth Rotation
Aperture Synthesis

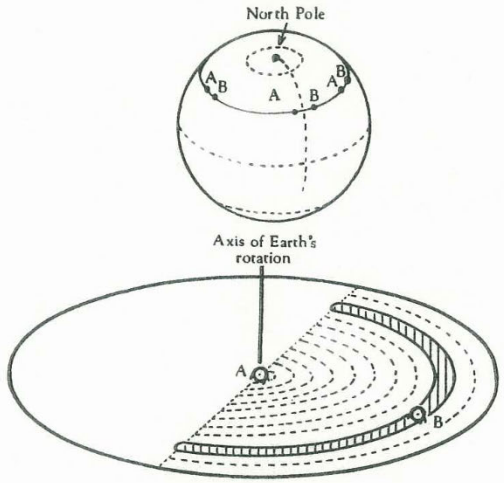

aperture
plane
coverage

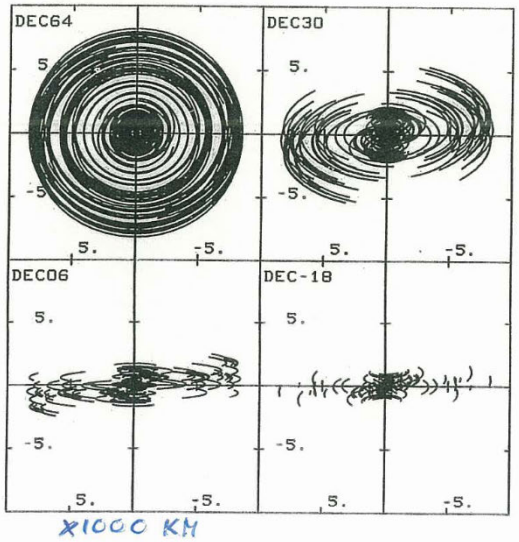

Sir Martin Ryle,
Nobel Prize in Physics, 1970

How (VLB) Interferometry works?

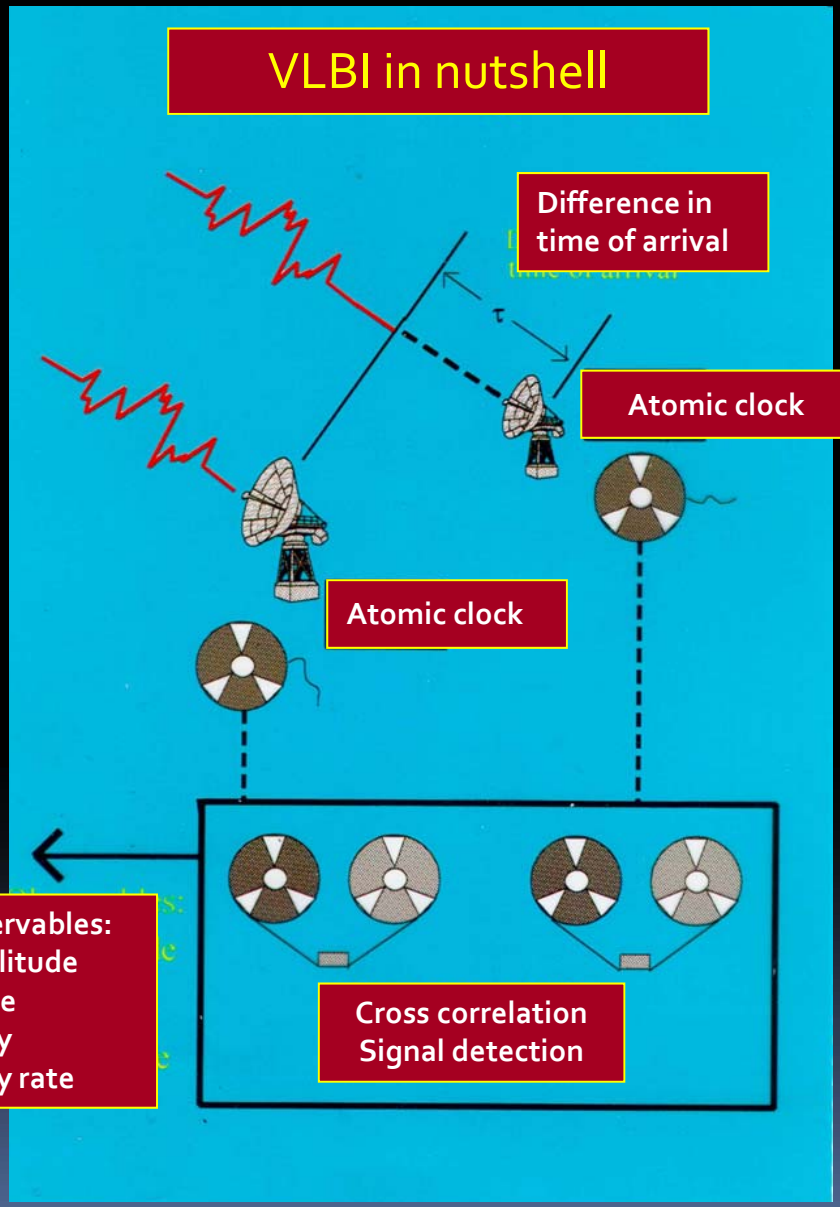

⇐ telescopes in different locations (countries, continents)

⇐ data relayed or recorded on magnetic media and transported to a central facility

⇐ data processed ("correlated")

Data rate: ~1 Gbps per RT;

Total: ~ 1-100 TB per experiment

JIVE: the heart of EVN

From recording to real-time VLBI: e-VLBI

- In line with ICT developments
- Boosted with EC FP6 EXPReS
  - *…and now continues with FP7 NEXPReS*
  - *Help solve last mile problem at telescopes*
  - *Work with NRENs on robust connectivity*
  - *Push to 1 Gb/s/telescope and beyond*
  - *Transition from EVN to e-EVN*
- Now an operational facility
  - *Guaranteed 10 x 24 h per year*
  - *Flexible ways to get into e-VLBI*
  - *Request e-VLBI for fast response*
  - *Or for triggered proposals*
  - *Short requests <2hr*
  - *Targets of Opportunities*
  - *Produces excellent science!*
- e-EVN – an SKA pathfinder

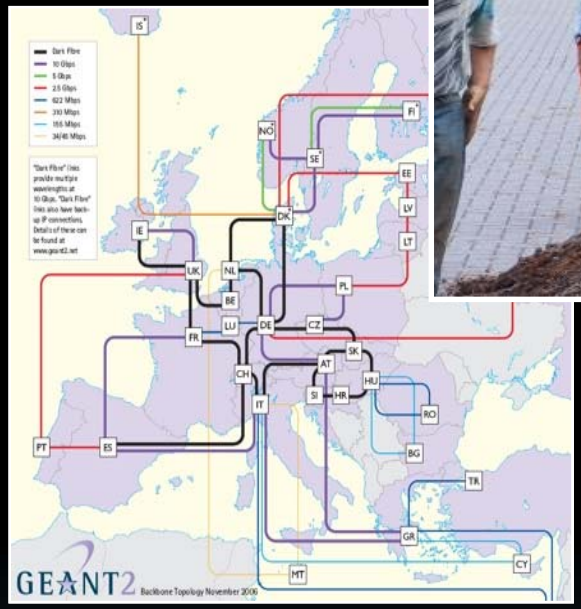

EXPReS

Express Production Real-time e-VLBI Service

e-VLBI: the end of “traditional” VLBI

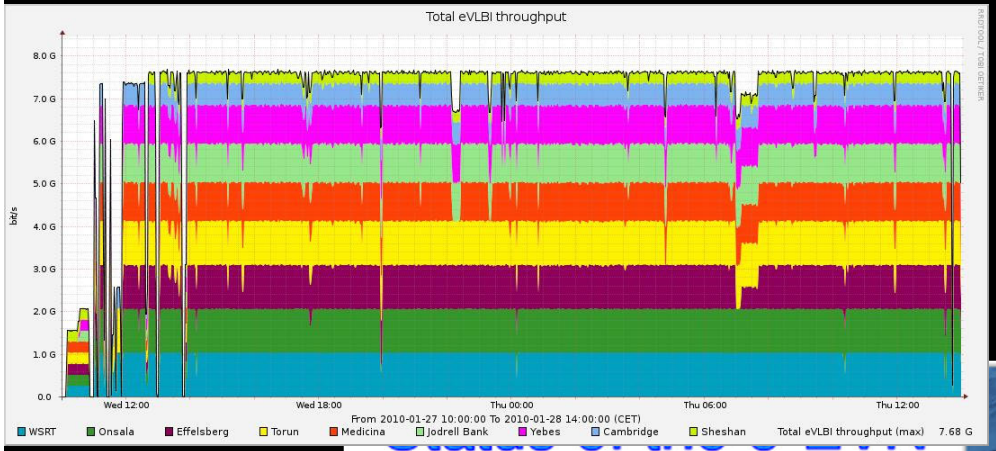

Feb 2010: uninterrupted 24 hours

e-EVN run with ~8 Gbps incoming rate

JOINT INSTITUTE FOR VLBI IN EUROPE

RADIO INTERFEROMETRIC IMAGING

OR

DOING THE MAGIC...

"Golden formulae" of interferometry & aperture synthesis

1. Van Cittert – Zernike theorem (optics analogy):

$$V(u,v) = \int_{-\infty}^{+\infty}\int_{-\infty}^{+\infty} I(x,y)e^{i2\pi(ux+vy)}dxdy$$

Visibility function

Brightness distribution

2. Correlation, convolution and Wiener-Khinchin theorem:

$$r(\tau) = \lim_{T\to\infty}\frac{1}{2T}\int_{-\infty}^{\infty} V_{1T}(t)V_{2T}^{*}(t-\tau)dt$$

$$V_{1T} \otimes V_{2T} \xleftrightarrow{Fourier} F(V_{1T})F(V_{2T}^{*})$$

Interferometric imaging basics

Interferometer response to a source of brightness distribution $I(l,m)$:

$$V(u,v,w) = \int\int A(l,m) I(l,m) e^{-2\pi i[ul+vm+w(\sqrt{1-l^2-m^2}-1)]} \frac{dl\ dm}{\sqrt{1-l^2-m^2}}$$

Ideally, in 2D-approximation:

$$\frac{A(l,m)I(l,m)}{\sqrt{1-l^2-m^2}} = \int\int V(u,v) e^{2\pi i[ul+vm]} du\ dv$$

Difficulties with the above integral:
- Incomplete sampling of the uv-plane;
- Errors, additive and multiplicative, in measuring $V(u,v)$

The first recipe of image reconstruction

1. FOURIER INVERSION

   Formation of an initial "dirty image" from the visibility samples collected from an interferometric array

2. DECONVOLUTION

   Correction of the effect of Fourier plane sampling deficiencies on the dirty image

3. SELF-CALIBRATION

   Correction of the effect of calibration errors on the deconvolved image

Fourier inversion 1

- We want $I(l,m) = \int V(u,v) e^{-2\pi i(ul+vm)} du dv$

(leaving out the $\frac{A(l,m)}{\sqrt{1-l^2-m^2}}$ term for convenience)

BUT

We measure noisy, poorly calibrated samples of the visibility function at discrete locations in the Fourier plane

- We can define a complex sampling function S(u,v) which is (1,0) where data was sampled and (0,0) elsewhere.

We replace V(u,v) by the sampled visibility function S(u,v)V(u,v)

where $S(u,v) = \sum_k w_k \delta(u-u_k)\delta(v-v_k)$ w_k = weight

Dirty imaging

- Then the image we obtain is

$$I^D(l,m) = \int S(u,v)V(u,v)e^{-2\pi i(ul+vm)}dudv$$

↑

Dirty image

or $$I^D(l,m) = \sum_k V(u_k,v_k)e^{-2\pi i(u_k l+v_k m)}w_k$$

The dirty image is a sum of harmonic functions with amplitudes and relative phases taken froim the visibility function (as measured).

Deconvolution

$I^D = F^{-1}(SV)$ = F.T. of sampled visibility function.

The Dirty Image, I^D, is not the true image of the sky since the sampled visibility is not the true visibility.

The Fourier convolution theorem states that the FT of the product of two functions is the convolution of the FTs of the two functions

So the Dirty Image is related to the True Image by

$I^D = B * I$
(the convolution of the true image, I, with a dirty beam B)

where $B = F^{-1}(S)$ i.e. $B(l,m) = \sum_k \cos[2\pi(u_k l + v_k m)] w_k$

Effect of uv-sampling

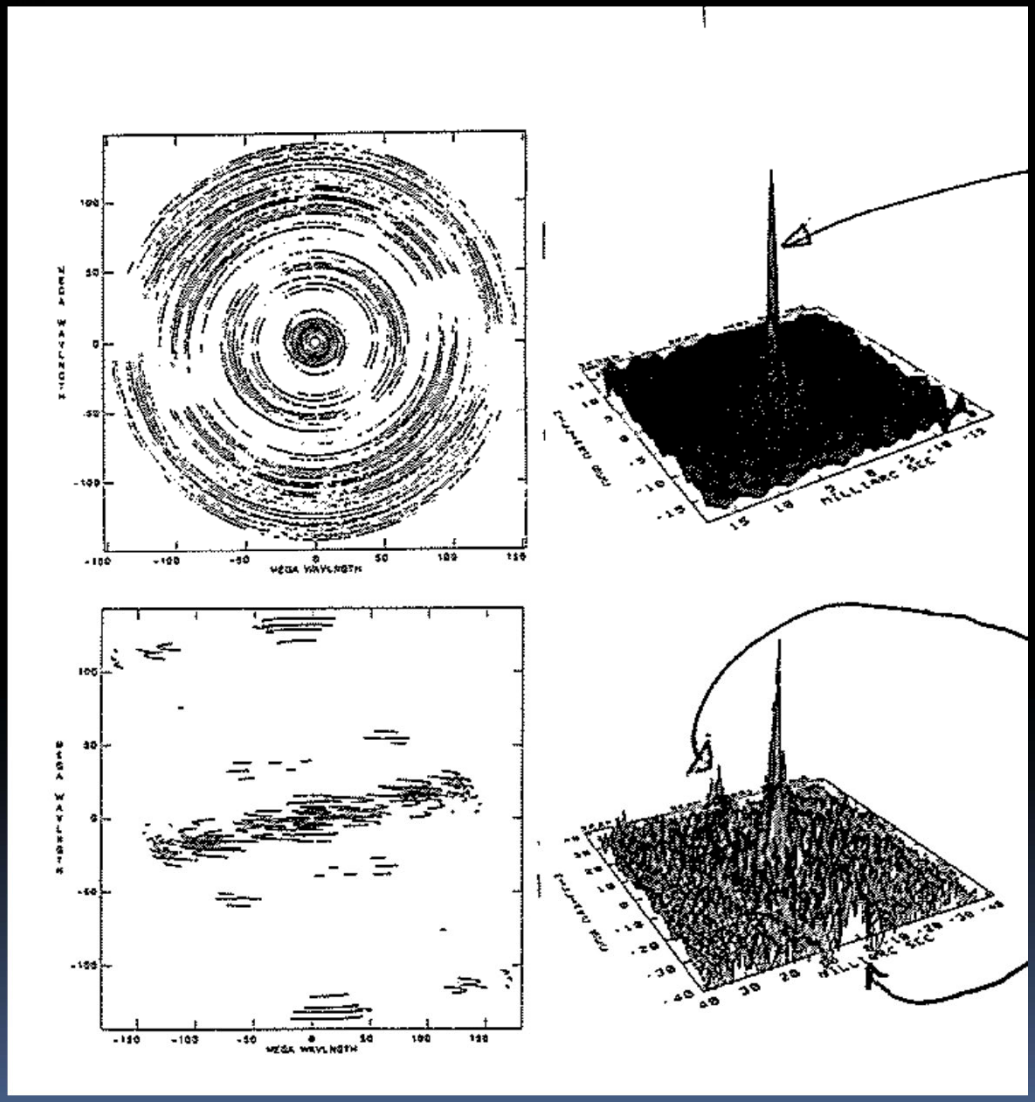

Good (dense) uv-sampling – small sidelobes

Bad (sparse) uv-sampling – large sidelobes

Deconvolution realities…

- Each point seen in the dirty image is a product of the true image feature (a delta-function with the correct amplitude) and the properly positioned and scaled dirty beam

when we write $I^D = B*I$, we are effectively doing the Fourier Transform assuming that there are zeroes at the places where we have no data. So there are many other solutions to this equation which are invisible.

B is composed of a finite number of sinusoids, so we can have many functions Z(l,m) that happen to have non-zero amplitude where B has a zero ie B*Z=0

To recover I(l,m) we need a non-linear deconvolution procedure since the FT of the Dirty Image is full of zeroes.

- The trick is to choose the most plausible combination of measured and "other" data, so that the deconvolution process makes sensible guesses about the behaviour of the visibility function between samples.

A-priori knowledge is always helpful…

1. emission is known or assumed to be non-zero only within a small area in the field of view. The sky is mostly empty. This called "finite support".

2. the emission is known to be positive, or the fractional polarization is known to be ≤ 1.

3. the sky is a collection of point sources

$$I^s = \sum_{i=1}^{p} I_i^D \delta(l - l_i)\delta(m - m_i)$$

I_s = solution of convolution equ.

4. the sky is smooth, e.g. image dispersion is minimal
   $\int I^2(l,m)dldm$ is minimal

(A glimpse on) UV-weighting

- Natural weighting helps to minimize the noise in the dirty image:

$$w_k = \frac{1}{\sigma_k^2}$$ (=> visibility samples are weighted by integration time)

- But, this results in "overweighting" the uv-areas with high sampling density (usually – near the origin); in turn it means "throwing out the baby" – long baselines are suppressed
- Uniform weighting is used to minimize the rms sidelobes of dirty beams i.e. correction for local sampling density):

$$w_k = \frac{1}{\rho(u_k, v_k)}$$

CLEAN (see TMS and references therein)

1. Find peak brightness in the dirty map
2. Position center of dirty beam (≡ synthesized beam pattern) on the peak in the dirty map
3. Multiply dirty beam with the amplitude of the peak times the "loopgain"
4. Subtract multiplied dirty beam from the dirty map
5. The residual map serves as the new dirty map in an iterative process
6. Iterate steps 1 to 5 until some cutoff level is reached
7. Convolve the 'clean' components with a 'clean beam' – a Gaussian function with FWHM=resolution of interferometer.
8. Add convolved clean components to the last residual map → clean image

Closure relations in VLBI

- Measurables: $V(u,v) \equiv A(u,v) \times \exp[i\varphi(u,v)]$

  but $\varphi_{\rm m}(u,v) = \varphi_t(u,v) + \varepsilon_\varphi(u,v,t);\ \ \varepsilon_\varphi(u,v,t) >> 1$

- Closure phase: $\Phi_{123} \equiv \varphi_{12} + \varphi_{23} + \varphi_{31}$

  Φ_{123} = invariant(instrumental effects)

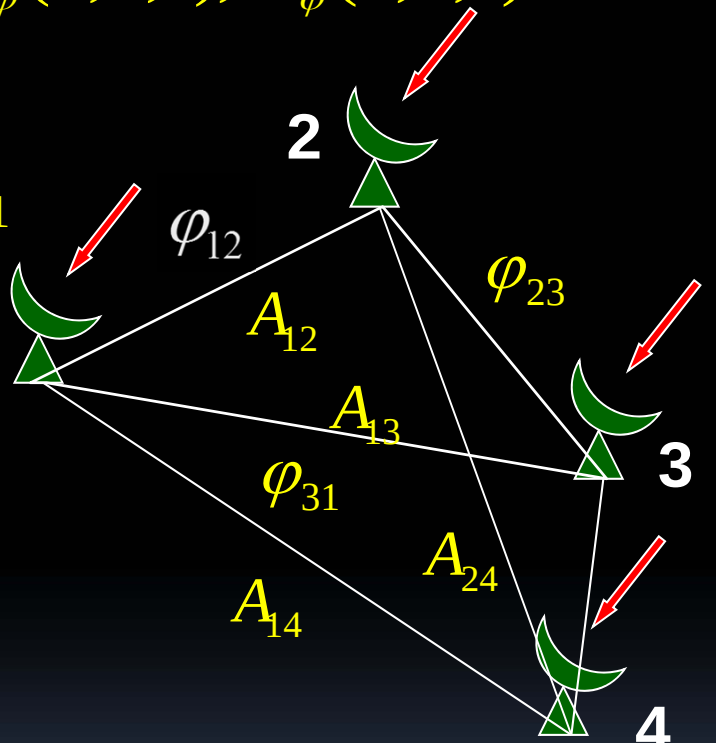

- Closure amplitude: $A_{1234} = \dfrac{A_{12}A_{34}}{A_{13}A_{24}}$

  A_{1234} = invariant(instrumental effects)

- *uv*-sampling ("*uv*-coverage") is incomplete

Vivat closure phase (Jennison, 1953)

- Closure phase is a good observable even in the presence of severe antenna-based errors, so long as the SNR is sufficient to define the visibility phase in the coherence time.

For an array with N antennas, there are $\frac{(N-1)(N-2)}{2}$ independent closure phases.

For large N, the number of linear combinations of baseline phase (≡ closure phases) ≈ number of baseline phases, so there is very little loss of information.

- Closure phase can be used in an iterative image estimation procedure

  (Readhead and Wilkinson 1978, Astrophysical Journal. 223, 35; Pearson and Readhead 1984, Ann. Rev. A&A 22, 97)

Practical recipe 2

1. choose initial model, I^{model}
2. predict visibilities for the model ; $V^{model} = F(I^{model})$
3. keep observed visibility amplitudes
4. select visibility phases by modifying model visibilities on some baselines to be consistent with the observed closure φ's
5. form new dirty image from new visibilities
6. form a new model I^{model} by e.g. CLEANing the new dirty image
7. go back to step 1) unless the process has converged

Recipe 3

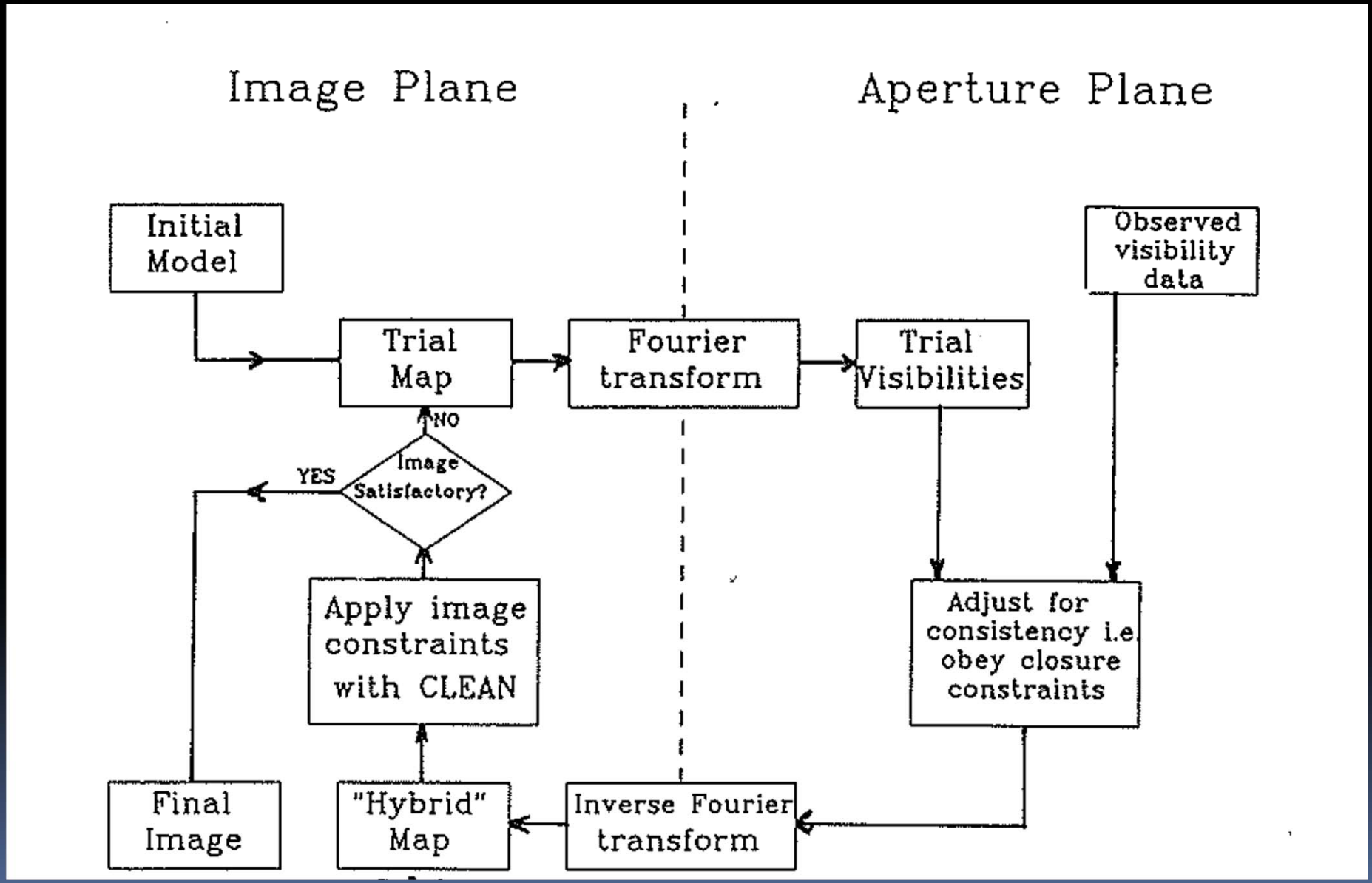
Image Plane
Aperture Plane
Initial Model
Trial Map
Fourier transform
Trial Visibilities
Observed visibility data
NO
YES
Image Satisfactory?
Apply image constraints with CLEAN
Adjust for consistency i.e obey closure constraints
Final Image
"Hybrid" Map
Inverse Fourier transform

Selfcalibration

Closure phase methods cancel antenna-based phase errors. Self-calibration methods estimate antenna-based phase errors and correct the visibility phases accordingly.

1. 2. 3. as for closure phase procedures
4. solve for the antenna phase errors using a least squares criterion (see later)
5. correct the observed visibilities for the antenna phase errors
6. form new dirty image from new visibilities
7. form new model I^{model} by e.g. CLEANing the new dirty image
8. go back to step 1 unless the process has converged

Example (from Wilkinson, VLBI Technologies, Felli & Spencer, 1989)

sampling function

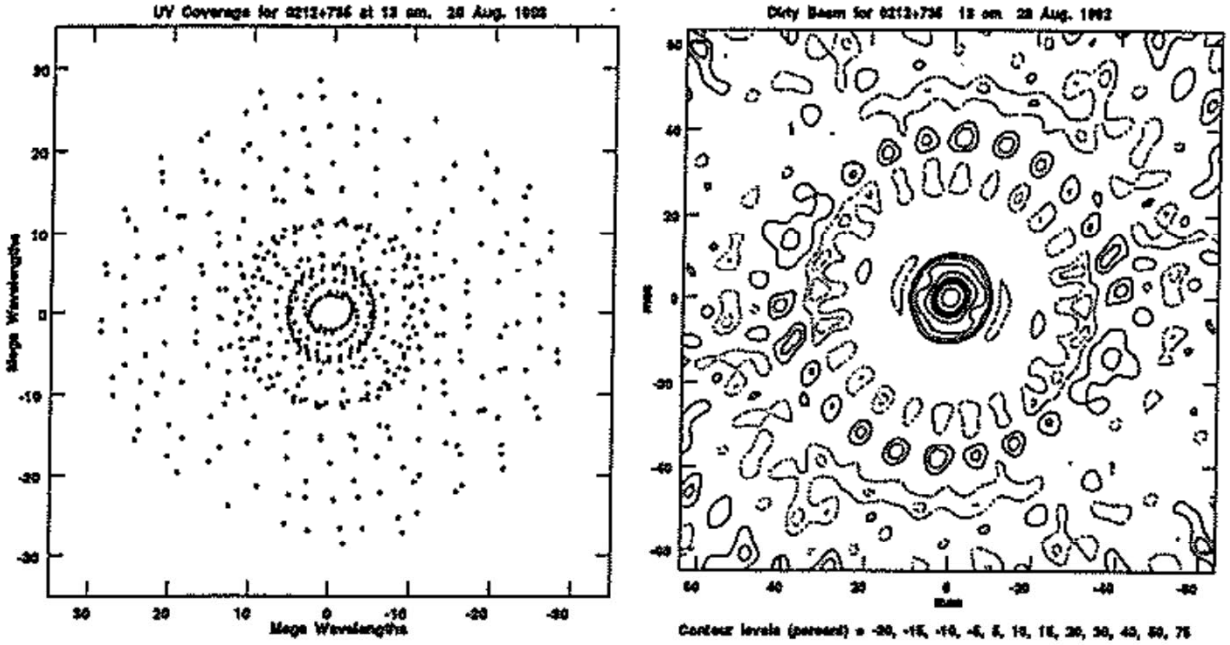

dirty beam

Figure 13.1: The (u, v) coverage and dirty beam for the example data set. This was 13 cm data on 0212+735 taken during a dual band (13 and 4 cm) geodesy experiment on the VLBA on 28 August 1993. The antennas involved were Hancock, North Liberty, Fort Davis, Pie Town, Kitt Peak, and Owens Valley (HN, NL, FD, PT, KP, OV).

Selfcalibration (hybrid mapping)

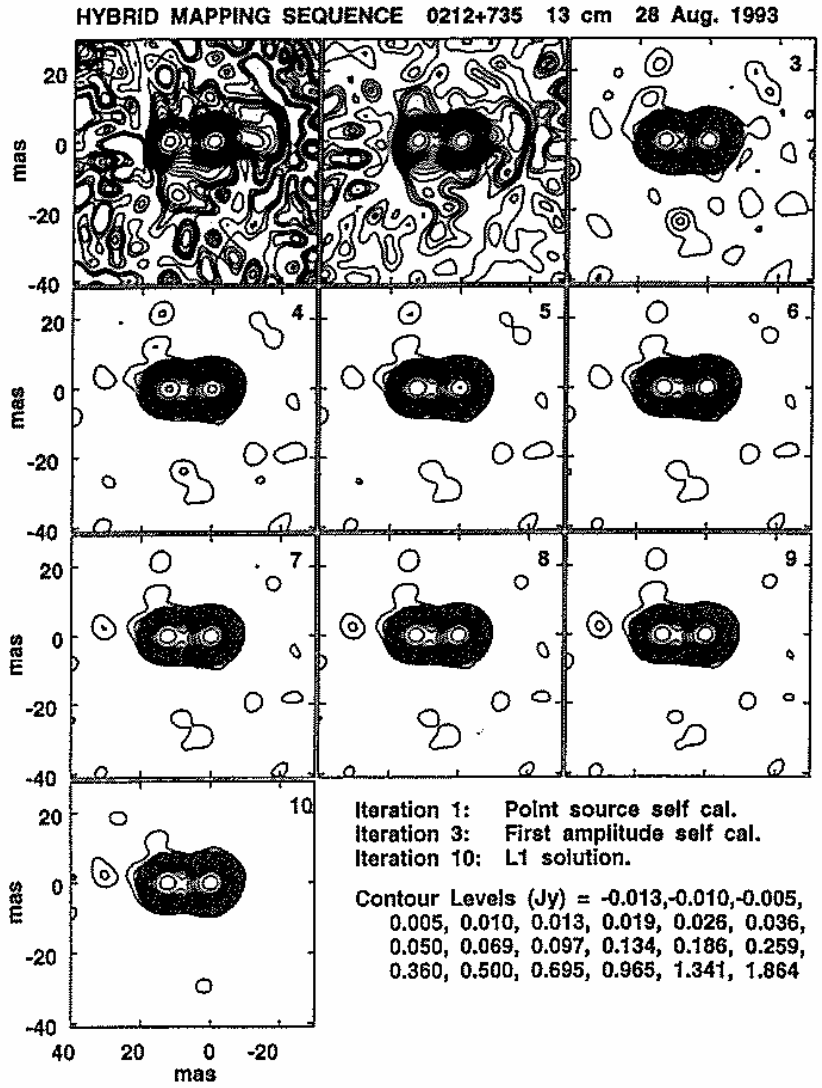

Figure 13.2: The hybrid mapping sequence on 0212+735. Good convergence, to an off-source rms noise level of 1.6 mJy was obtained in 10 iterations. The peak flux density in the final image is 1.75 Jy.

Is a reconstructed image unique?

Incomplete u-v coverage can lead to non-unique images – i.e. the convolution/deconvolution process has too many degrees of freedom

Can be checked using fake data from a model source. Errors in the difference maps are concentrated in the region where there is emission on scales equivalent to those not sampled by the uv coverage.

The off-source noise level is not a good measure of errors in the relative strength of regions with emission.

Solution is to provide dense uv coverage, no big holes

How does look the final product (of continuum VLBI)

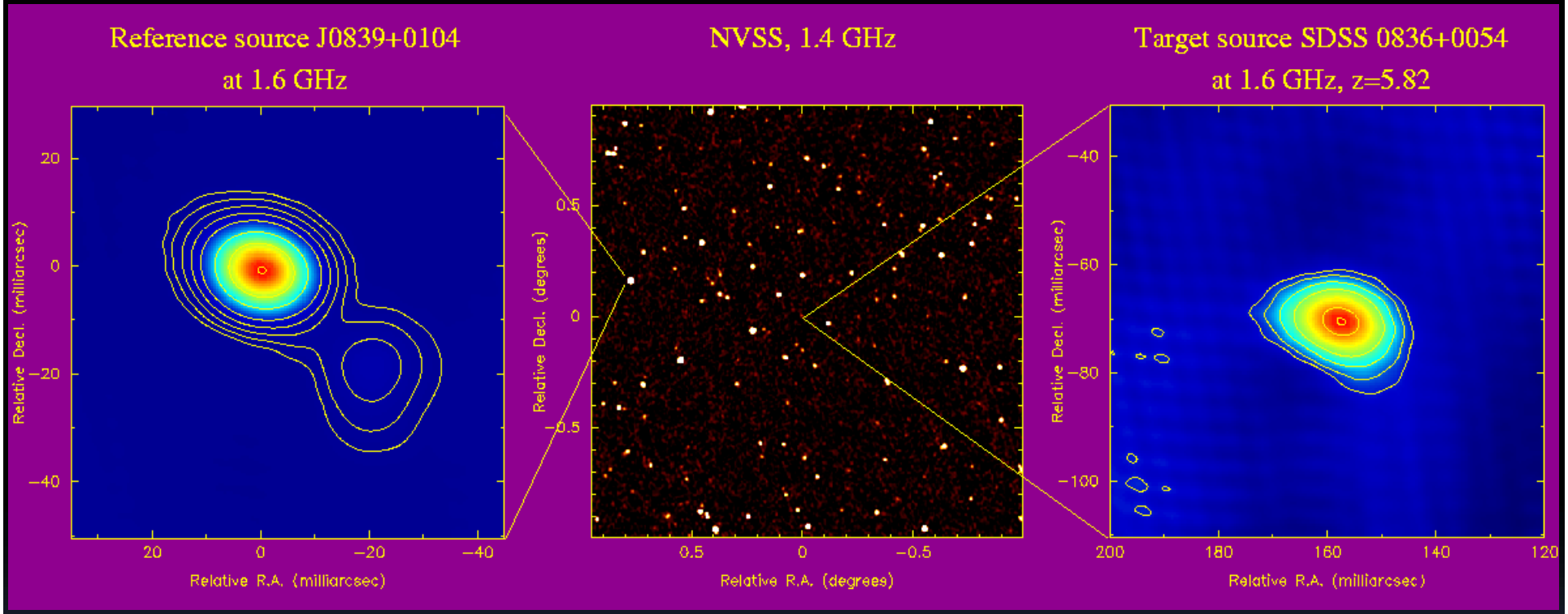

The weakest EVN target detected to date: $S_{1.4}$ = 1.1 mJy
VLBI image (right panel): 770 μJy/beam

Frey et al, 2003, 2005, MNRAS

VLBI imaging practice

- Exercise it; theoretical VLBI imaging is pointless
- Available software packages:
  - Astronomical Imaging Processing System (AIPS), supported by National Radio Astronomy Observatory (NRAO)
  - Differential Mapping softare (Difmap), supported (voluntarily) by CalTech
- Both packages are free (requires registration)
- Get your hands-on experience!

***Ya. Zeldovich*: "What's the use to study 'for the future'? Find a problem and solve it; this way you will learn something for real."**

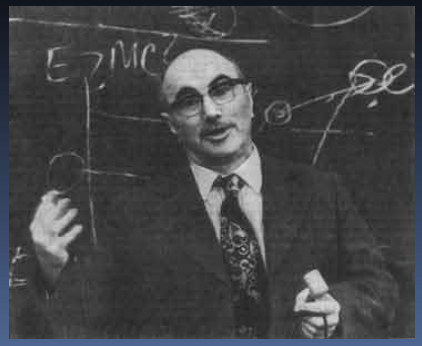

Useful reading on radio interferometry

- B. Burke, F. Graham-Smith
  An introduction to Radio Astronomy

- A.R. Thompson, J.M. Moran,
  G.W. Swenson, Interferometry and
  Synthesis in Radio Astronomy

- Radio Astronomy from Karl Jansky
  to Microjansky,
  eds. L.I. Gurvits, S. Frey, S.Rawlings
  EDP Sciences, 2005

- K. Rohlfs, T.L. Wilson
  Tools of Radio Astronomy